Available online at www.sciencedirect.com
ScienceDirect
Materials Chemistry and Physics 109 (2008) 360–364
MATERIALS CHEMISTRY AND PHYSICS
www.elsevier.com/locate/matchemphys

Mechanical properties of InGaN thin films deposited by metal-organic chemical vapor deposition

Sheng-Rui Jian [a,*], Jason Shian-Ching Jang [a], Yi-Shao Lai [b], Ping-Feng Yang [b], Chu-Shou Yang [c], Hua-Chiang Wen [d], Chien-Huang Tsai [e]

[a] *Department of Materials Science and Engineering, I-Shou University, Kaohsiung 840, Taiwan*
[b] *Central Labs, Advanced Semiconductor Engineering, Kaohsiung 811, Taiwan*
[c] *Department of Electrophysics, National Chiao Tung University, Hsinchu 300, Taiwan*
[d] *Department of Mechanical Engineering, National Chung Cheng University, Chia-Yi 621, Taiwan*
[e] *Department of Automation Engineering, Nan Kai Institute of Technology, Nantou 54243, Taiwan*

Received 6 April 2007; received in revised form 6 October 2007; accepted 1 December 2007

Abstract

We report in this study characteristics of InGaN thin films developed by metal-organic chemical vapor deposition (MOCVD) at various growth temperatures. The effect of deposition temperatures on microstructures and mechanical properties are examined using X-ray diffraction (XRD), scanning probe microscopy (SPM), and nanoindentation techniques. The XRD analysis shows no evidence of phase separation for InGaN thin films. The SPM micrographs indicate that the films have relatively smooth surfaces. Hardness and Young's modulus of InGaN thin films vary according to the deposition temperature. As the deposition temperature increases from 730 to 790 °C, the grain size increases from 28 to 52 nm. Hardness for InGaN thin films dropped from 13.8 to 17.6 GPa in accordance with the increase of the grain size. By fitting experimental data with the Hall–Petch equation, a probable lattice friction stress of 3.48 GPa and Hall–Petch constant of 73.15 GPa $nm^{1/2}$ are obtained.

PACS: 61.10.Nz; 62.20.−x; 68.37.Ps

Keywords: Nanoindentation; InGaN; XRD; MOCVD

1. Introduction

Tremendous progresses in the research and development of wide-band-gap GaN and related III-nitride materials have attracted a great deal of attention due to their potential applications in optoelectronic and electronic devices in the UV–vis range [1]. In contrast, research on their mechanical properties has not drawn an equal attention. In addition to optical and electrical properties, mechanical properties of these materials are crucial in the device design, in particular when reliability issues concerning delamination, brittle fracture, and fatigue degradation of the thin film structures become major concerns.

Various methods, including atomic force microscopy [2], impulse acoustic method [3], and Brillouin light scattering [4], have been developed for measuring the mechanical properties of thin films. Among these methods, the nanoindentation technique is capable of providing a nondestructive measurement of film properties without being affected by the substrate. Nanoindentation has been widely used for measuring elastic modulus, E, and hardness, H, of small volumes of materials and thin films [5–11]. The load–displacement responses obtained during nanoindentation also provide substantial insights into the mode and onset of plastic deformations or fracture of a material [12,13].

The growth and characteristics of InGaN thin films deposited by metal-organic chemical vapor deposition (MOCVD) at various growth temperatures were investigated in this study. Microstructural properties of the deposited films were characterized by X-ray diffraction (XRD) while the surface morphology by scanning probe microscopy (SPM). The effect of deposited temperatures on microstructures and mechanical properties (hardness and elastic modulus) are discussed as well.

2. Experimental details

Experimentally, InGaN thin films were grown on sapphire substrates by the horizontal low-pressure MOCVD method. Prior to materials growth, the

* Corresponding author. Tel.: +886 7 6577711x3130; fax: +886 7 6578444.
E-mail address: srjian@gmail.com (S.-R. Jian).

0254-0584/$ – see front matter © 2007 Elsevier B.V. All rights reserved.
doi:10.1016/j.matchemphys.2007.12.007

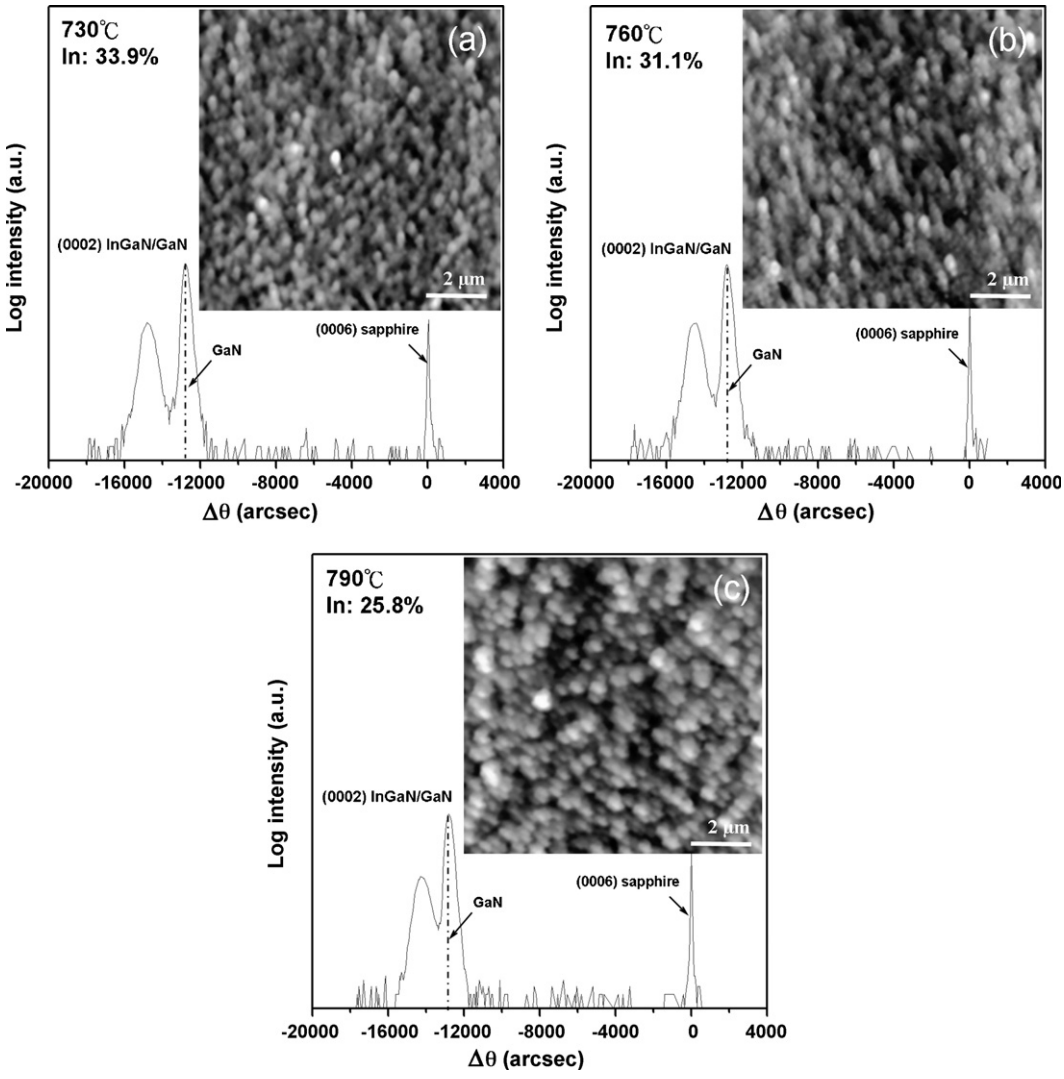

Fig. 1. X-ray diffraction analysis for InGaN thin films deposited at the various growth temperatures of 730, 760 and 790 °C for the indium content of (a) 33.9 at.%, (b) 31.1 at.% and (c) 25.8 at.%, respectively. Inserts: corresponding topography images measured by dynamic force microscopy.

sapphire substrates were annealed and cleaned to remove surface residual stress and impurities in hydrogen gas at 1120 °C for 10 min. Trimethylgallium (TMGa), trimethylindium (TMIn), and ammonia (NH_3) were used as the source precursors for gallium, indium and nitrogen, respectively. At first, a 25-nm thick GaN nucleation layer was deposited onto the sapphire substrate at 520 °C for 4 min. The substrate temperature was then raised to 1120 °C to grow a 2-μm thick undoped GaN layer. A 500-nm thick InGaN thin film was grown on this undoped GaN layer. During the development of the InGaN thin film, the reactor pressure was kept constant at 200 mbar and input flow rates of ammonia, TMGa, and TMIn were set at 12, 26.5 and 25.5 μmol min^{-1}, respectively. To obtain various indium concentrations, the deposition temperature was varied from 730 to 790 °C. Indium concentration in the deposited thin films was examined by separating GaN and InGaN peaks in the XRD spectra following Vegard's law [14].

The crystalline structure of the deposited InGaN films was characterized using a Bede QC200 X-ray diffractometer with Cu Kα irradiation at 40 kV and 0.4 mA. SPM systems (SPI4000 & SPA300HV, Seiko) with a Si cantilever (SI-DF3, Seiko), which has a spring constant of 11 N m^{-1} and a free resonance frequency of 125 kHz, were employed to observe the morphology of InGaN thin films. Tests were carried out under the dynamic force microscopy (DFM) mode, which features a greater resolution than the conventional atomic force microscopy (AFM) mode.

Nanomechanical characterizations of MOCVD deposited InGaN thin films were conducted using a Nano Indenter XP instrument (MTS Cooperation, Nano Instruments Innovation Center, TN, USA). Nanoindentation measurements, using a diamond Berkovich indenter tip (tip radius ∼50 nm), were conduced under the CSM mode, which was accomplished by superimposing a small oscillation on the force signal and measuring the displacement response at the same frequency at 75 Hz. The indenter was loaded and unloaded three times to ensure that the tip was properly in contact with the surface of the sample to eliminate parasitic phenomena from the measurements. The indenter was loaded for the fourth and final time at a strain rate of 0.05 s^{-1}, with a hold period of 30 s at the peak load. After that the indenter was unloaded to 10% of the peak load. Ten indentations were performed for each sample and the results presented here stand for the averages. The indentations were sufficiently separated at 50 μm to avoid mutual interactions. We followed the analytic method developed by Oliver and Pharr [15] to determine the hardness and Young's modulus of InGaN thin films from their load–displacement curves.

3. Results and discussion

XRD spectra and topography images of MOCVD derived InGaN thin films deposited at various growth temperatures are

illustrated in Fig. 1. The InGaN and GaN peaks are present in the spectra and these two peaks do not shift significantly as the indium concentration increases. Indium concentrations in InGaN thin films deposited at 730, 760 and 790 °C are 33.9, 31.1, and 25.8 at.%, respectively. Broadness of the InGaN peak is attributed to alloying and finite domain size effects [16].

Fig. 1 also shows typical DFM images of MOCVD derived InGaN thin films developed at 730, 760 and 790 °C. These thin films exhibit dense microstructures with homogeneous grain sizes and smooth film surfaces. Average surface roughness and grain size of InGaN thin films determined from the DFM images are shown in Fig. 2. As the deposition temperature increases from 730 to 790 °C, i.e., the indium concentration decreases from 33.9 to 25.8 at.%, the average grain size of InGaN thin films increases from 28 to 52 nm, which leads to the increasing of the average surface roughness from 2.71 to 6.65 nm. This is because with the increase of the deposition temperature, mobility of the surface atoms increases, resulting in larger grain size and surface roughness.

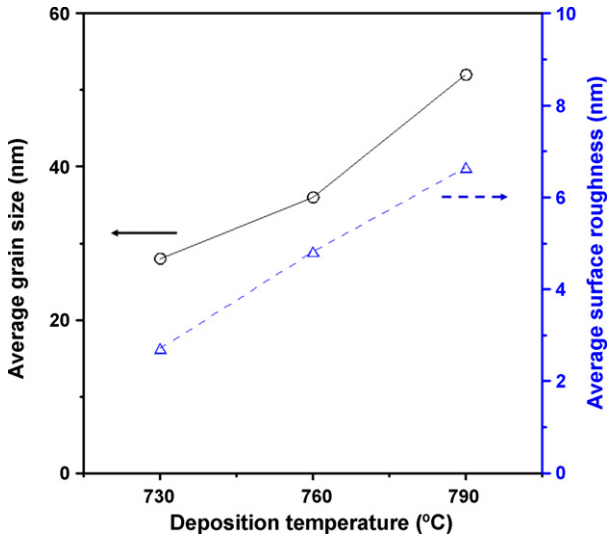

Fig. 2. The deposition temperature dependence of the average grain size and surface roughness for InGaN thin films.

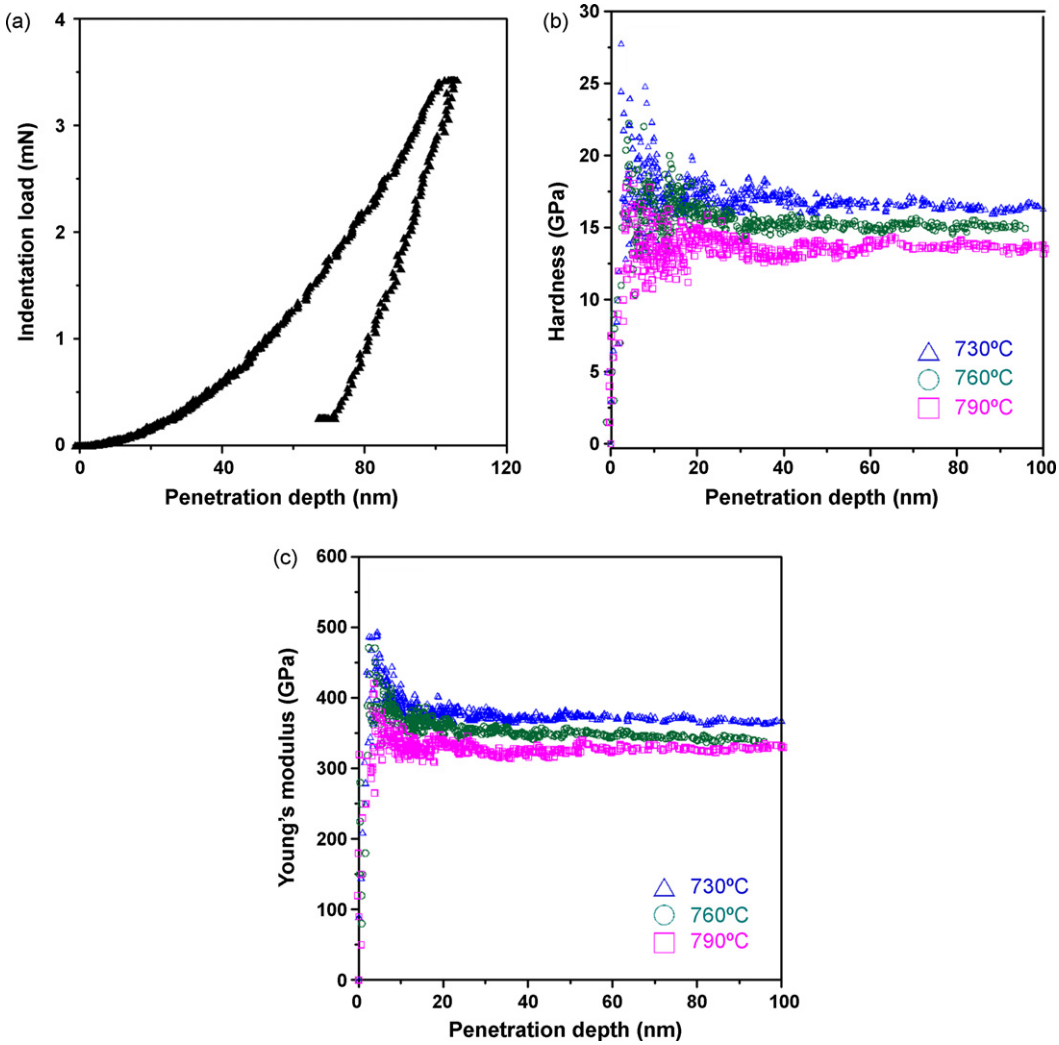

Fig. 3. Nanoindentation test results: (a) a typical load–displacement curve for InGaN thin film deposited at 730 °C; (b) hardness–displacement curves and (c) Young's modulus–displacement curves for InGaN thin films.

Results of nanoindentation measurements are displayed in Fig. 3. A typical load–displacement curve for the InGaN thin film deposited at 730 °C is shown in Fig. 3(a). The total penetration depth into the InGaN thin film was 100 nm with a peak load between 3.5 and 4 mN. Hardness and Young's modulus of InGaN thin films can be calculated from the load–displacement data [15]. The hardness is estimated by

$$H = \frac{P_{\max}}{A_c} \tag{1}$$

where $P_{\max}$ is the peak load and A_c is the contact projected area, which is determined by the geometry of the indenter and the contact depth, h_c. It is assumed that the indenter geometry can be described by an area function $F(h_c)$. In this work, the area of contact is described as [15]

$$A_c = F(h_c) = 24.69h_c^2 + 122.80h + 212.77h_c^{1/2} - 191.25h_c^{1/4} - 32.77h_c^{1/8} \tag{2}$$

The elastic modulus is determined from the following relation:

$$E_{\text{eff}} = \frac{1}{2\beta} S \sqrt{\frac{\pi}{A_c}} \tag{3}$$

where S and β are denoted as the measured stiffness and a shape constant of 1.034 for a Berkovich indenter. The E_{eff} is the effective elastic modulus defined by

$$\frac{1}{E_{\text{eff}}} = \frac{1-\nu_f^2}{E_f} + \frac{1-\nu_i^2}{E_i} \tag{4}$$

which takes into account the fact that elastic displacements occur in both the thin film and indenter. The elastic modulus E_i and Poisson's ratio ν_i of the Berkovich indenter used in this work are 1150 GPa and 0.07, respectively. The Poisson's ratio of the thin film is assumed to be 0.3. Combining Eqs. (3) and (4), one can obtain the Young's modulus of the thin films, E_f, as follows:

$$E_f = \frac{(1-\nu_f^2) S E_i \sqrt{\pi}}{2\beta E_i \sqrt{A_c} - (1-\nu_i^2) S \sqrt{\pi}} \tag{5}$$

Through the continuous contact stiffness measurement, the displacement dependence of hardness and Young's modulus, as shown in Fig. 3(b) and (c), can be obtained.

Hardness versus penetration depth curves for InGaN thin films deposited at various growth temperatures are displayed in Fig. 3(b). A clear trend can be observed from the figure that the hardness decreases as the deposition temperature increases. It is well known that the hardness of a material depends on the grain size. The influence of the grain size on the hardness is described by the Hall–Petch equation [17]:

$$H = H_i + k_{\text{H–P}} d^{-1/2} \tag{6}$$

where H_i, d and $k_{\text{H–P}}$ are denoted as the lattice friction stress, the grain size, and the Hall–Petch constant, respectively. This implies that the hardness becomes lower as the grain size increases. Since a higher deposition temperature leads to a greater grain size for the InGaN thin films, it is reasonable to consider that the decrease of hardness is a result of an enlarged grain size. To characterize the grain size effect of hardness in InGaN thin films, the hardness at a penetration depth of 30–100 nm is regarded as the hardness of the sample because the hardness at a small depth may not be accurate owing to the tip calibration, surface roughness, and property inhomogeneities [18], while that at a large depth may involve the substrate effect. The hardness versus $d^{-1/2}$ data of InGaN thin films deposited at various growth temperatures are shown in Fig. 4. As shown in this figure, the hardness drops from 17.6 GPa for InGaN thin film deposited at 730 °C with an average grain size of 28 nm to 13.8 GPa for InGaN thin film deposited at 790 °C with an average grain size of 52 nm. The dashed line plotted in Fig. 4 stands for curve fitting of experimental results based on the Hall–Petch equation:

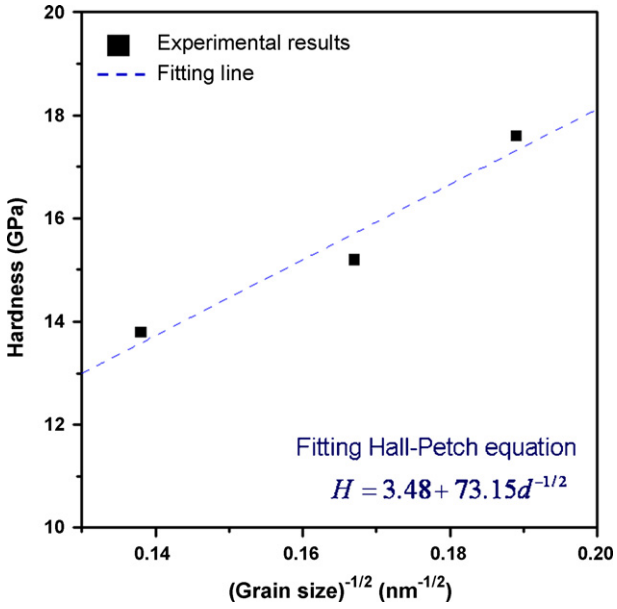

Fig. 4. Experimental results of hardness vs. grain size fitted by the Hall–Petch equation.

$$H = 3.48 + 73.15d^{-1/2} \tag{7}$$

which indicates a probable lattice friction stress of 3.48 GPa and a Hall–Petch constant of 73.15 GPa nm$^{1/2}$ for InGaN thin films.

The penetration depth dependence of Young's modulus is shown in Fig. 3(c). Similar to hardness, Young's modulus varied according to the deposition temperature as well as the penetration depth. Based on the Young's modulus at a penetration depth of 30–100 nm, InGaN thin film deposited at 730 °C exhibits the highest value of 374.3 GPa, while the InGaN thin film deposited at 790 °C the lowest one of 327.8 GPa.

4. Conclusion

The XRD, SPM, and nanoindentation with a Berkovich indenter tip were used to investigate microstructures as well as mechanical characteristics of MOCVD derived InGaN thin films deposited at various growth temperatures.

In summary, XRD measurements showed that there was no phase separation of indium as the indium composition went from 25.8 to 33.9 at.%. Investigated by SPM, grain size and surface roughness of InGaN thin films both increase as the deposition temperature increases. Results indicate that the hardness decreases as the deposition temperature increases: 17.6 GPa for 730 °C to 13.8 GPa for 790 °C. On the other hand, the highest Young's modulus of 374.3 GPa appear at the deposition temperature of 730 °C, while the lowest one of 327.8 GPa at 790 °C. The experimental data fitted by a Hall–Petch equation show a probable lattice friction stress of 3.48 GPa and a Hall–Petch constant of 73.15 GPa $nm^{1/2}$ for the InGaN thin films.

Acknowledgement

This work was partially supported by the National Science Council of Taiwan, under Grant No.: NSC 96-2112-M-214-001.

References

[1] E.T. Yu, III–V nitride semiconductors: applications and devices, in: M.O. Manasreh (Ed.), Optoelectronic Properties of Semiconductors and Superlattices, vol. 16, Taylor & Francis, New York, 2003.
[2] S. Chowdhury, M.T. Laugier, Nanotechnology 15 (2004) 1017.
[3] D.C. Hurley, V.K. Tewary, A.J. Richards, Thin Solid Films 398 (2001) 326.
[4] P. Djemia, C. Dugautier, T. Chauveau, E. Dogheche, M.I. De Barros, L. Vandenbulck, J. Appl. Phys. 90 (2001) 3771.
[5] F. Kokai, M. Taniwaki, M. Ishihara, Y. Koga, Appl. Phys. A 74 (2002) 533.
[6] S.R. Jian, T.H. Fang, D.S. Chuu, J. Electron. Mater. 32 (2003) 496.
[7] X.D. Li, H. Gao, C.J. Murphy, K.K. Caswell, Nano Lett. 3 (2003) 1495.
[8] X.D. Li, X. Wang, Q. Xiong, P.C. Eklund, Nano Lett. 5 (2005) 1982.
[9] V.A. Coleman, J.E. Bradby, C. Jagadish, P. Munroe, Y.W. Heo, S.J. Pearton, D.P. Norton, M. Inoue, M. Yano, Appl. Phys. Lett. 86 (2005) 203105.
[10] D. Pan, T.G. Nieh, M.W. Chen, Appl. Phys. Lett. 88 (2006) 161922.
[11] D. Lee, S. Jia, S. Banerjee, J. Beck, I.P. Herman, J.W. Kysar, Phys. Rev. Lett. 98 (2007) 026103.
[12] H. Bei, Z.P. Lu, E.P. George, Phys. Rev. Lett. 93 (2004) 125504.
[13] S.J. Bull, J. Phys. D: Appl. Phys. 38 (2005) R393.
[14] Z. Qin, Z. Chen, Y. Tong, S. Lu, G. Zhang, Appl. Phys. A 74 (2002) 655.
[15] W.C. Oliver, G.M. Pharr, J. Mater. Res. 7 (1992) 1564.
[16] R.W. Vook, in: J.W. Matthews (Ed.), Epitaxial Growth, Academic, New York, 1975.
[17] R. Venkatraman, J.C. Bravman, J. Mater. Res. 7 (1992) 2040.
[18] M.S. Bobji, S.K. Biswas, J.B. Pethica, Appl. Phys. Lett. 71 (1997) 1059.